TOPICAL COLLECTION: INTERNATIONAL CONFERENCE ON THERMOELECTRICS 2019

Investigation of Thermoelectric Properties of $Ag_2S_xSe_{1-x}$ (x = 0.0, 0.2 and 0.4)

SAURABH SINGH [ID],[1,3,5] KEISUKE HIRATA,[1] DOGYUN BYEON,[1] TAKUYA MATSUNAGA,[1] OMPRAKASH MUTHUSAMY,[1] SWAPNIL GHODKE,[1] MASAHIRO ADACHI,[2] YOSHIYUKI YAMAMOTO,[2] MASAHARU MATSUNAMI,[1] and TSUNEHIRO TAKEUCHI[1,3,4]

1.—Research Center for Smart Energy Technology, Toyota Technological Institute, Nagoya 468-8511, Japan. 2.—Sumitomo Electric Industries Ltd., Hyogo 664-0016, Japan. 3.—CREST, Japan Science and Technology Agency, Tokyo 102-0076, Japan. 4.—Institute of Innovation for Future Society, Nagoya University, Nagoya 464-8603, Japan. 5.—e-mail: saurabhsingh@toyota-ti.ac.jp

Materials best-suited for direct application exhibit a high thermoelectric figure of merit (ZT) close to unity, from room temperature to ~ 400 K. In this work, we investigated the thermoelectric behavior of Ag_2Se, and a sulfur substituted Ag_2Se system, i.e. $Ag_2S_{0.2}Se_{0.8}$ and $Ag_2S_{0.4}Se_{0.6}$, in the temperature range of 300 K to 500 K. With strong anharmonic lattice vibration and semiconducting electronic structure, these materials showed thermal conductivity less than 1 W m^{-1} K^{-1}, electrical resistivity ~ 1 mΩ cm, together with moderate Seebeck coefficient values of ~ -140 μV K^{-1} in the low-temperature phase. We were able to achieve ZT equal to unity in a wide temperature range of 350–400 K, with a maximum value of ZT = 1.08 at 350 K for the $Ag_2S_{0.4}Se_{0.6}$ material.

Key words: Thermoelectrics, silver chalcogenides, phase-transition

INTRODUCTION

Consumption of the energy resources is increasing at a very fast rate due to tremendous demand. The main contributors to fulfil the requirements are coal, oil, and natural gas. These resources are natural, and limited;[1] therefore, alternate sources of energy are highly desirable, which could not only reduce our dependence on natural energy sources, but could also decrease global warming.

In the search for possible solutions, thermoelectric generators are one of the most interesting technologies by which a large amount of unused waste heat can be converted into useful electric energy.[2–4] A workable thermoelectric generator demands thermoelectric materials possessing good thermoelectric properties leading to a high value of the *dimensionless-figure-of-merit* (ZT), defined as $ZT = S^2\sigma T\kappa^{-1}$, where S is the Seebeck coefficient, σ is electrical conductivity, T is the absolute temperature, and κ is thermal conductivity, which includes both electron (κ_e) and lattice contributions (κ_l).[5,6] From the formula for ZT, one can see that high values of Seebeck coefficient and electrical conductivity along with lower thermal conductivity are required to obtain a larger value of ZT. The interdependence of S, σ and κ_e imposed by carrier density make it challenging to achieve high ZT. In addition to the magnitude, the temperature at which a material possesses high ZT is also very important, as waste heat is available in a wide temperature range from room temperature (body heat) to thousands of degrees Celsius (vehicles exhaust and industrial plants).[7,8] It should be emphasized that a huge amount of unused waste heat (home appliances, body heat, electronic devices, etc.) is available in the temperature range below 100°C, and it is easily accessible by humans in daily life. Thus, materials with large ZT in these

temperature ranges are highly desirable for a variety of applications.

In the past several decades, different classes of thermoelectric (TE) materials have been extensively investigated to achieve high values of ZT.[9] Among various classes of TE materials studied so far, chalcogenides, A_2X (where A=Ag, Cu and X=S, Se, Te) have attracted much attention due to their low thermal conductivity and semiconducting electronic structure.[10–15] Although their superionic conduction in the high-temperature phase is not good for thermoelectric applications, these materials can be suitable for applications as electrolyte materials in making fuel cells.[16] The effects of the superionic state becomes more pronounced with temperature, thus it is not appropriate to consider this material for thermoelectric applications in a high-temperature region. Improvement in the value of ZT for the better thermoelectric applications in low-temperature regions, can be possible by decreasing the material's electrical resistivity. As a result, one can create a possible candidate among the chalcogenides suitable for consideration as a thermoelectric material.

In the low-temperature phase of this type of material, the lower κ value is favorable toward obtaining a large ZT. In addition to the lower value of κ; large values of Seebeck coefficient (S) and electrical conductivity (σ) are required to get a larger value of power factor (PF = $S^2\sigma$).

Recently, Byeon et al.[17] discovered a self-tuning of carrier concentration-effect which led to a colossal value of $S^2\sigma$ = 2.3 W m^{-1} K^{-2} and a colossal value of ZT (= 470) in a Cu_2Se compound. However, the very large ZT value was limited to a small temperature range; in practical application, it needed further modification to extend the large value of ZT to a wider temperature range in a similar type of system.

Among the several possible combinations of A_2X (X=S, Se, Te), the Ag_2S material has also been investigated extensively due to its non-toxicity and small band gap ($\sim$ 1.0 eV), which make it very useful for vast applications such as photovoltaic devices and IR detectors with nano-structuring sample synthesis.[18–20] In addition to these applications, Ag_2S shows very low thermal conductivity ($\sim$ 0.5 W m^{-1}K^{-1}), and a large negative Seebeck coefficient ($\sim$ – 900 μV K^{-1}).[19] In the low temperature phase, i.e. monoclinic structure below 450 K, Ag_2S shows very high electrical resistivity ($\sim$ 3.2 $\times$ 10^7 mΩ cm at 300 K).[19] Despite its low thermal conductivity and high Seebeck coefficient, the large electrical resistivity of this material prevented us from obtaining a large ZT in the low temperature phase. Suppression of electrical resistivity from 10^7 mΩ cm to a few mΩ cm is a very challenging task, as it requires the introduction of large carrier concentration without increasing the total thermal conductivity.

Another material in the A_2X group is Ag_2Se, which has been studied from thermoelectric aspects as it has the narrow band gap semiconductor with E_g = 0.07 eV at 0 K, has electrical resistivity $\sim$ 1 mΩ cm and low thermal conductivity of $\sim$ 1 W m^{-1} K^{-1}.[14,21,22] Ag_2Se undergoes phase transition from the β-Ag_2Se (orthorhombic) low-temperature phase to the α-Ag_2Se (cubic) ionic conductor high-temperature phase at about 407 K.[21,22] Various studies on thermoelectric properties of this material in bulk and thin films have been reported in recent years.[14,21–25] The highest ZT = 0.96 about room temperature for the bulk sample is reported by Ferhat et al,[11] with a large power factor equal to 3.5 mW m^{-1} K^{-2} and low thermal conductivity $\sim$ 0.96 W m^{-1} K^{-1}. Most recently, Yang et al.[22] reported a systematic investigation by different synthesis techniques to achieve a large value of ZT; the maximum value reported for the bulk sample was 1.2 at 390 K. Perez-Taborda et al.[23] also reported a very large power factor $\sim$ 2.44 mW m^{-1} K^{-2} on a thin film sample made by using the pulse hybrid magnetron synthesis technique, a very costly method. Room temperature chemical synthesis, a relatively inexpensive synthesis method, was carried out by Ding et al;[24] a flexible film on nylon membrane was reported with a large power factor of 0.987 mW m^{-1} K^{-2}.

The previous study shows that, with sulfur substitution on selenium sites of Ag_2Se, a significant drop in the phase transition temperature occurs until the composition $Ag_2S_{0.4}Se_{0.6}$, and increases further with an increase in sulfur content.[25] Thus, we believe that owing to the same valance charge of sulfur and selenium, the transition temperature can be lowered with sulfur substitution and a high ZT can be obtained at a much lower temperature without much effect on its electrical resistivity. Also, to the best of our knowledge, the effect of sulfur substitution in Ag_2Se systems has not been investigated from the thermoelectric perspective. Therefore, in this study we investigated sulfur concentration dependence of thermoelectric properties for $Ag_2Se_{1-x}S_x$ in the low-temperature phase by making samples at x = 0, 0.2, and 0.4. With sulfur substitution, we found that a high ZT equal to 1.08 was obtainable at 350 K for the $Ag_2S_{0.4}Se_{0.6}$, which is a much lower temperature (at least 40 K lower) than 390 K as reported with ZT = 1.2.[22] Having ZT = 1.08 at just 50 K above the room temperature is one of the main outcomes of the present research. This characteristic would cover most of the humanly-generated waste heat sources for electrical energy conversion with a very inexpensive material and technique.

EXPERIMENTAL PROCEDURES

To synthesize the polycrystalline samples, we used a self-propagating high-temperature synthesis (SHS) technique for Ag_2Se, whereas a melting

method (MM) was used for $Ag_2S_xSe_{1-x}$ ($x = 0.2$ and 0.4). The melting method is very effective for making high quality, homogeneous sulfur substituted samples, as in the SHS method sulfur evaporates (due to its relatively lower melting temperature) before the reaction with selenium is complete. Materials in powdered form, silver (Ag, purity 3N), sulfur (S, 4N), and selenium (Se, 3N) were mixed in stoichiometric ratios, using mortar and pestle for ~ 20 min until homogeneous. In the case of SHS method, the homogenized powder was cold pressed into pellet form, and then reacted on an electrically heated tantalum plate under vacuum conditions. In the melting method, on the other hand, the homogenized powder was sealed in an evacuated quartz tube and heated at $1000°C$ for 12 h, followed by furnace cooling to room temperature.

A highly dense sample in pellet form was made by an additional hot-press technique. In the hot-press method, a pressure of ~ 40 MPa was used. Sintering temperature varied sample to sample, as each sample had a different composition. Thus, we monitored the displacement parameter during the sintering process, and from the saturation point the sintering time was held for next 15 min.

Structural characterization of as-prepared powder sample was carried out by using a Bruker D8 Advance with a Cu K_α x-ray source. The morphology and mapping analysis of sintered samples were conducted by scanning electron microscope (SEM) using a JEOL JSM-6330F and energy-dispersive x-ray spectroscopy (EDX) using a JED-2140GS with the accelerating voltage of 20 kV, respectively. The composition was analyzed by electron probe micro analysis (EPMA) using a JEOL JXL-8230. Heat and electron transport properties were measured on hot-pressed, dense bulk samples. Density measurement was done by using the Archimedes principle. Thermal conductivity measurement was done by using laser flash analysis (NETZSCH LFA 457). Seebeck coefficient and electrical resistivity were measured using experimental systems developed in our laboratory.[17]

RESULTS AND DISCUSSION

The room temperature x-ray diffraction (XRD) pattern for $Ag_2S_{1-x}Se_x$ ($x = 0$, 0.2 and 0.4) is shown in Fig. 1a. For structural phase confirmation, XRD data of all the compositions were analyzed by using the Rietveld refinement method implemented in the FullProf Suite software.[26,27] The XRD patterns of all the samples were found to be in single-phase, and free from any secondary phases. The Miller indices of the XRD peaks corresponding to the Bragg reflection positions, shown in Fig. 1a, were associated with the orthorhombic crystal structure phase (space group No. 19—$P2_12_12_1$) for the Ag_2Se and $Ag_2S_{0.2}Se_{0.8}$ samples, but with monoclinic phase (space group No. 14—$P2_1/c$) for the $Ag_2S_{0.4}Se_{0.6}$

sample.[28–34] The results from Rietveld refinement are shown in Fig. 1b, and we obtained good fit for all the compositions. The refined lattice parameters, atomic positions, R-factor, and goodness of fit are given in the supplementary tables S1–S3 (see supplementary Tables S1–S3). In the present study, the values of lattice parameters obtained from Rietveld refinement were found to be in good agreement with the literature.[29] The density values obtained from Archimedes methods were 8.13, 7.98, and 7.65 g/cc^3, for Ag_2Se, $Ag_2S_{0.2}Se_{0.8}$, and $Ag_2S_{0.4}Se_{0.6}$, respectively. The measured density was greater than the 96% of the theoretical density. Figure 2 shows the surface morphology and composition distribution of Ag_2Se, $Ag_2S_{0.2}Se_{0.8}$, and $Ag_2S_{0.4}Se_{0.6}$. It indicates that all sample surfaces were very smooth with distribution of homogeneous composition. From the EPMA measurement, the averaged chemical compositions were found to be $Ag_{1.961 \pm 0.015}Se_{1.038 \pm 0.014}$, $Ag_{1.979 \pm 0.012}S_{0.182 \pm 0.008}Se_{0.839 \pm 0.010}$, and $Ag_{1.992 \pm 0.012}S_{0.382 \pm 0.008}Se_{0.626 \pm 0.011}$, corresponding to the nominal composition of Ag_2Se, $Ag_2S_{0.2}Se_{0.8}$, and $Ag_2S_{0.4}Se_{0.6}$, respectively. The EPMA analysis revealed that the measured compositions were very similar with respective to their nominal compositions. The compositions of all samples were summarized in the supplementary Tables S4–S6 (see Supplementary Tables S4–S6).

Purposefully, we carried out thermoelectric measurements in a wide temperature range for a better comparison of obtained results between low temperature and high temperature phases of each composition.

Temperature dependence of electrical resistivities (ρ) for all the samples are shown in Fig. 3a. Below the structural phase transition temperature (T_p), all the compositions show monotonically decreasing behavior of ρ with increasing temperature. In addition, a small increase in magnitude was observed for $Ag_2S_{0.4}Se_{0.6}$ in the temperature range from 300 K to 315 K. This type of temperature-dependent behavior is certainly unusual, but similar behavior was reported previously for Ag_2Se.[21,25] Below T_p, temperature-dependent behavior for $x = 0.0$ and 0.2 was found to be similar, but for the $x = 0.4$ case it was different. Also, a big change in T_p for $x = 0.4$ was observed, which suggests that sulfur substitution played a key role in changing the T_p value. The shift in value of T_p towards lower temperature followed a systematic decreasing trend with increase in sulfur concentration. The values of T_p for Ag_2Se, $Ag_2S_{0.2}Se_{0.8}$, and $Ag_2S_{0.4}Se_{0.6}$ were found to be 404 K, 363 K, and 353 K, respectively. Above T_p, all compositions showed similar behaviors, with rather small variations observed in their magnitudes and their temperature-dependence.

For sulfur substituted composition, the electrical resistivity suddenly dropped with increasing temperature at T_p, while the electrical resistivity for Ag_2Se increased across the phase transition with
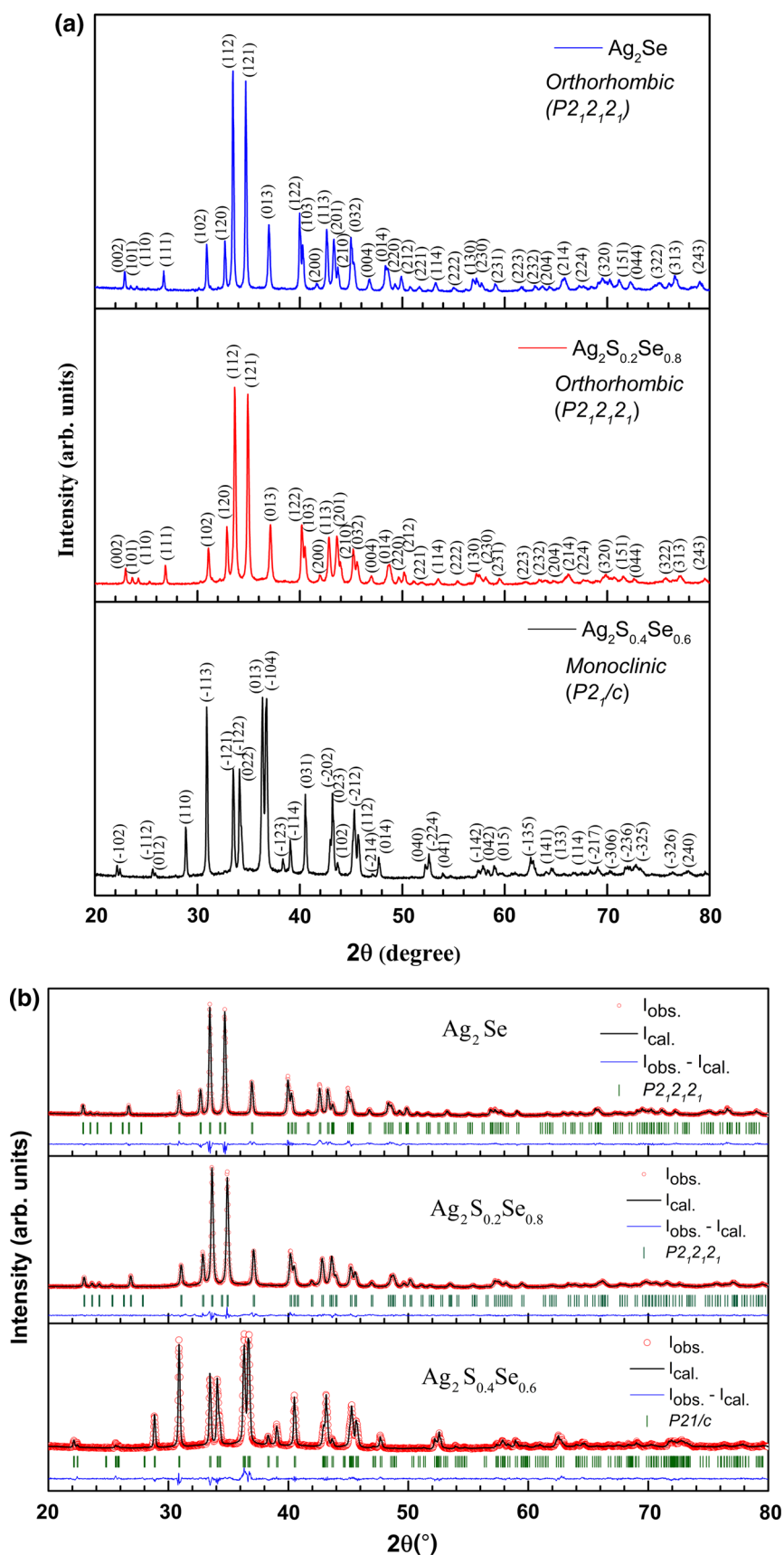
Fig. 1. Shown are (a) x-ray diffraction patterns for Ag_2Se (top), $Ag_2S_{0.2}Se_{0.8}$ (middle), $Ag_2S_{0.4}Se_{0.6}$ (bottom) (b) Rietveld refinement analyses for Ag_2Se (top) and $Ag_2S_{0.2}Se_{0.8}$ (middle), $Ag_2S_{0.4}Se_{0.6}$ (bottom).
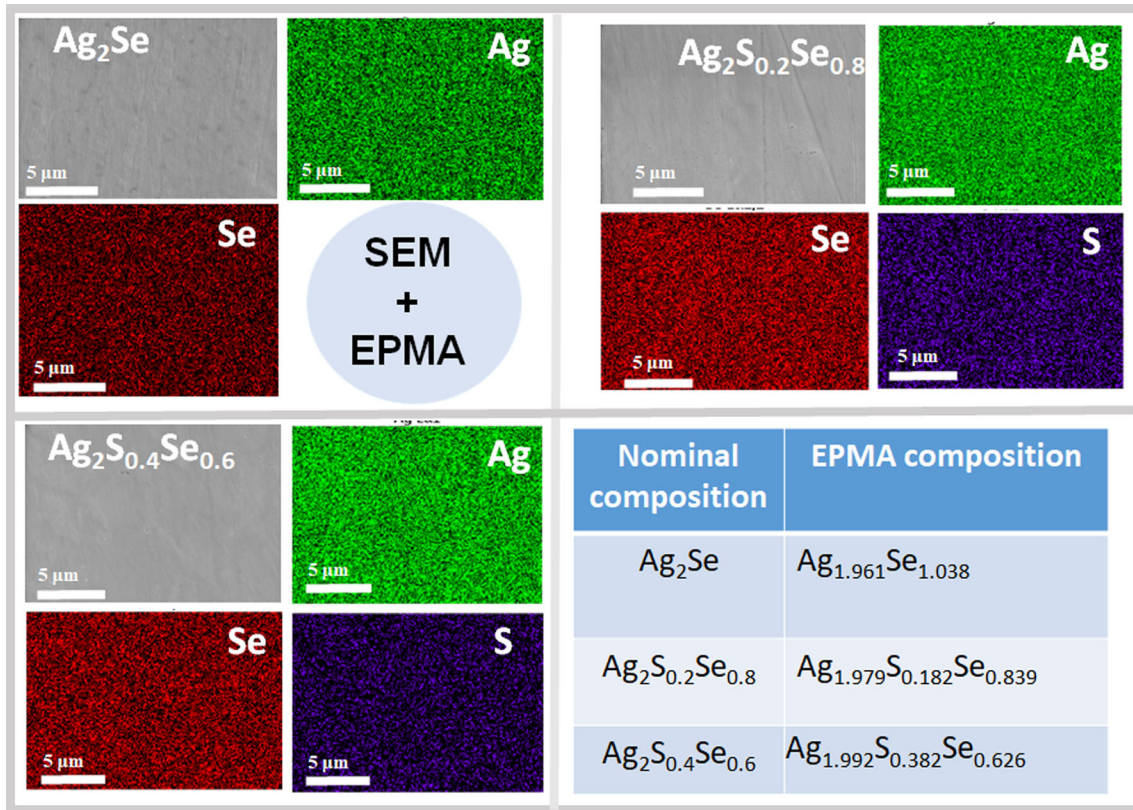
Fig. 2. SEM mapping and EPMA analyses for Ag_2Se, $Ag_2S_{0.2}Se_{0.8}$, and $Ag_2S_{0.4}Se_{0.6}$ compositions.

increasing temperature. In the low-temperature region below the phase transition, the temperature dependence of electrical resistivity in Ag_2Se was similar to that of semiconducting materials. However, at about 407 K, it transformed into the α-Ag_2Se, which is known as a superionic conductor. At the transition temperature, the magnitude of electrical resistivity suddenly increased, presumably because of the increase of scattering probability of electrons and/or the decrease of conduction electrons. The former is related to the structure disordering in association with superionic conduction, in which the positions of Ag ions dynamically change. The latter is caused by decrease of excess Ag or increase of deficient Se, both of which lead to a decrease of conduction electrons.

At 300 K, the value of ρ for Ag_2Se was observed to be ~ 1.1 mΩ cm. At this temperature, earlier reported values for Ag_2Se systems were 0.5–1.42 mΩ cm by Ferhat et al., ~ 1.54 mΩ cm by Ding et al., ~ 0.5 mΩ cm by Yang et al., and 1.75–2.5 mΩ cm by Pei et al.[11,21,22,24] Quantitatively, the value of ρ decreased from 1.1 mΩ cm to 0.83 mΩ cm when x was equal to 0.2. This change is not very prominent, as with such an amount of sulfur substitution, crystal structure remains orthorhombic, and the change in electronic conduction is not significantly large. However, for the $Ag_2S_{0.4}Se_{0.6}$ composition, the value of resistivity at 300 K was found to be ~ 1.71 mΩ cm, which is

nearly 1.5 times the value observed for $x = 0$. The change in electrical resistivity can be attributed to the decrease in carrier concentration due to Se deficiency, as discussed earlier. Thus, at room temperature, the Seebeck coefficient for $Ag_2S_{0.4}Se_{0.6}$ compositions is expected to possess higher magnitude than that of Ag_2Se and $Ag_2S_{0.2}Se_{0.8}$.

The order of magnitude of the observed ρ for all the compositions falls into the category of good thermoelectric materials whose typical range is from a few to 10 mΩ cm.

Seebeck coefficients (S) of all three samples were measured and their temperature dependent behaviors are plotted in Fig. 3b. All compositions show negative S in the entire temperature region under investigation, suggesting that electrons make the dominant contributions to the transport properties. At 300 K, both Ag_2Se and $Ag_2S_{0.2}Se_{0.8}$ show almost the same magnitude of S, as the values of resistivity for these compositions are nearly the same, whereas we found relatively higher magnitude of $S(300\ K) = -184\ \mu V\ K^{-1}$ for $Ag_2S_{0.4}Se_{0.6}$, in good consistency with the slightly higher electrical resistivity.

For Ag_2Se, the value of S at room temperature is $\sim -142\ \mu V/K$, which is very similar to the previously reported values on bulk samples.[22,24] The values of S for Ag_2Se are very sensitive to the sample synthesis conditions, as slight deviations in chemical compositions result in significant changes

in the carrier concentrations. Therefore, sample synthesis methods and heat treatments given prior to the transport measurement have key roles in determining the thermoelectric properties of these systems. The magnitude of S at 300 K reported by Ferhat et al.[11] stayed in the range from $-113\ \mu V\ K^{-1}$ to $-155\ \mu V\ K^{-1}$, depending upon the carrier concentration. Recently, Yang et al.[22] investigated the role of synthesis conditions on thermoelectric properties of Ag_2Se, and reported that the values of S at 300 K for cold press samples and melting-cooling spark plasma sintering (SPS) methods were $-135\ \mu V/K$ and $-105\ \mu V/K$, respectively. In comparison to these previously reported values, the magnitude of the non-substituted sample in our study was $-142\ \mu V/K$ at 300 K, which is a reasonable value, as in the present study the pellet was prepared using the hot-press method. Similar to the resistivity, the magnitude of S decreases with temperature and shows an electronic transition at structural phase transition temperature.

In the low temperature phase region, each composition shows a higher magnitude of Seebeck coefficient than that of its corresponding high

temperature phase. Above the phase transition temperature of each composition, the magnitude of S was also found to exhibit a weak temperature dependence, which could be accounted for by the fact that change in resistivity with temperature has a very small variation.

The values of T_p from Seebeck measurements are in good agreement with those observed from the resistivity measurements. For the x = 0.4 case, a large decrement in value of T_p (= 350 K) is observed.

The power factor ($PF = S^2\sigma$) was calculated from S and σ, and the resulting values were plotted in Fig. 3c as a function of temperature. Interestingly, we found a significant increase of PF regardless of composition in the low temperature phase, which is mainly due to a decrease in electrical resistivity while maintaining the large magnitude of the Seebeck coefficient. The maximum PF was found for the $Ag_2S_{0.2}Se_{0.8}$ sample, with a magnitude of $5.0\ mW\ m^{-1}\ K^{-2}$ at 360 K, which is largest value ever reported for the Ag_2Se based chalcogenide material. For the Ag_2Se sample, the maximum PF previously reported was $3.5\ mW\ m^{-1}\ K^{-2}$ at 300 K by Ferhat et al.[11] In our study, for the Ag_2Se system
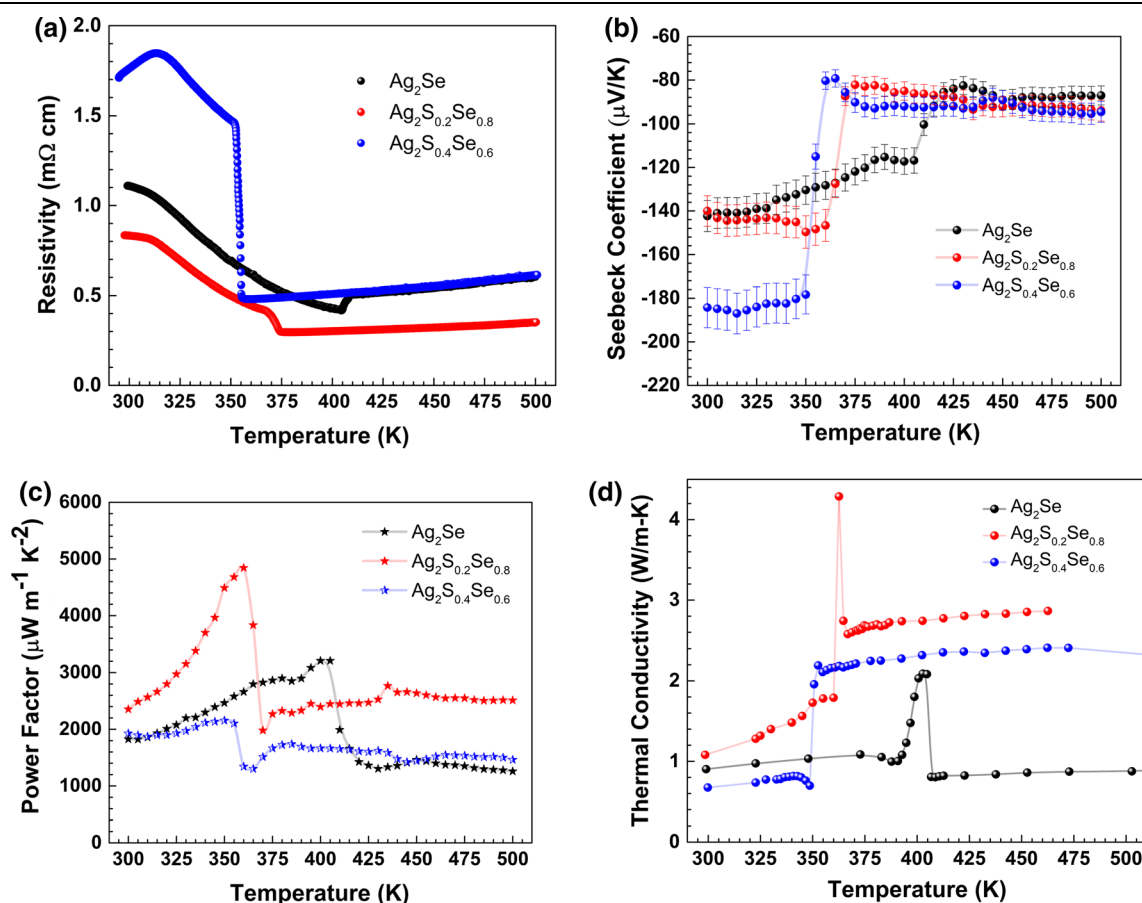

Fig. 3. Shown are (a) electrical resistivity (ρ) variation with temperature, (b) Seebeck coefficient (S) variation with temperature. (c) power factor (PF) variation with temperature, (d) thermal conductivity (κ) variation with temperature.
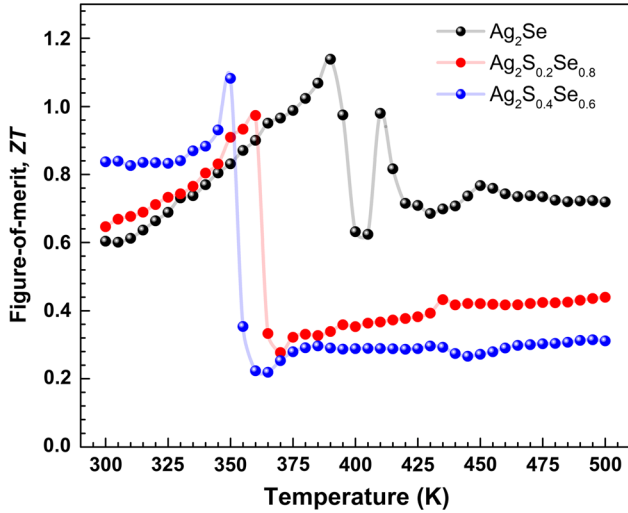
Fig. 4. Variation of *figure-of-merit, ZT* with temperature.

we found the peak in *PF* to be about 400 K with magnitude of 3.2 mW m^{-1} K^{-2}. Although the Seebeck coefficient values in the low temperature phase was relatively larger for Ag$_2$S$_{0.4}$Se$_{0.6}$, the values of PF were found to be nearly the same as that of Ag$_2$Se.

In the high temperature phase, *PF* was found to possess a very weak temperature dependence due to the weak temperature dependences both in Seebeck coefficients and electrical resistivity. Even though the magnitude of *PF* is lower in the high temperature phase than in the low temperature phase, the values of PF in the range of 1.2–2.5 mW m^{-1} K^{-2} are reasonably good for the thermoelectric materials. The main concern for these materials in the high temperature phase is their superionic conduction. The ionic charge carriers accumulate at the end of the material upon the electrical current. A serious heterogeneity in chemical composition would be generated in the material to be degraded. Thus, the high temperature phase cannot give good performance for long durations. Therefore, these materials are recommended to be used with large *PF* in the low temperature phase below T_p.

The thermal conductivities (κ) of all the samples were plotted as a function of temperature in Fig. 3d. Each sample possessed a sharp jump in magnitude of κ at the phase transition temperature. The low temperature phase showed relatively lower magnitudes of κ than their corresponding magnitudes in the high temperature phase. This is a very favorable result, for all the compositions to attain the high values of *ZT* in low temperature phase. At 300 K, the value of κ for Ag$_2$Se and Ag$_2$S$_{0.2}$Se$_{0.8}$ was nearly 1.0 W m^{-1} K^{-1}, whereas for the Ag$_2$S$_{0.4}$Se$_{0.6}$, it was much smaller, equal to $\sim$ 0.6 W m^{-1} K^{-1}. In the case of Ag$_2$Se, the magnitudes of κ in both the low

temperature phase and the high temperature phase were almost the same, due most likely to the similar value of electrical resistivity in both phases. Above phase transition, the value of κ remained almost temperature-independent for all the compositions, which can be attributed to the lack of significant change in carrier concentration.

We noticed a peak in κ at about T_p, which is attributed to the change in specific heat associated with the structural phase transition from β-Ag$_2$Se to α-Ag$_2$Se. The appearance of a peak at T_p was found for the Ag$_2$Se and Ag$_2$S$_{0.2}$Se$_{0.8}$ cases, however, for the Ag$_2$S$_{0.4}$Se$_{0.6}$ composition we did not notice any peak in κ. On the other hand, for the sulfur substituted composition, the sudden rise in κ above phase transition temperature was due to the contributions from electronic thermal conductivity (κ_e).

We also found an interesting feature in the variation of κ just below the phase transition temperature (10–15 K range below T_p) for Ag$_2$Se and Ag$_2$S$_{0.4}$Se$_{0.6}$ samples. The magnitude of κ decreases continuously and attains its minimum value before the phase transition takes place. Taken together, the peak in *PF* and minimum in κ below the T_p constitute a very favorable condition to achieve a large magnitude of *ZT*. The phase transition temperature obtained for each composition from the κ measurement is in good agreement with the T_p observed from electrical resistivity and Seebeck coefficient measurements. In addition to the magnitude, the systematic shift in T_p towards lower temperature upon sulfur substitution in Ag$_2$Se is also consistent.

Combining PF and thermal conductivity, we calculated the *ZT* value. The temperature-dependent variation of *ZT* is shown in Fig. 4. As we expected, *ZT* of all samples increased with increasing temperature, and eventually reached a peak at T_p. Above T_p, the value of *ZT* dropped down due to an increase in the κ. This trend in magnitude of *ZT* was also consistent with the *PF* behavior, and these behaviors were similar to those recently reported for Ag$_2$Se by Yang et al.[22]

The maximum values of *ZT* for Ag$_2$Se, Ag$_2$S$_{0.2}$Se$_{0.8}$ and Ag$_2$S$_{0.4}$Se$_{0.6}$ were found to be 1.14, 0.97, and 1.08, respectively. The temperatures at which the maxima in *ZT* occur are 390 K for Ag$_2$Se, 360 K for Ag$_2$S$_{0.2}$Se$_{0.8}$, and 350 K for Ag$_2$S$_{0.4}$Se$_{0.6}$.

In comparison to the maximum *ZT* reported by Yang et al., i.e. ZT_{max} = 1.2 for the cold press sample at 390 K, and ZT_{max} = 0.98 for the SPS sample, we found the ZT_{max} equal to 1.14 at 390 K by making a sample using a melting-cooling hot-press sintering technique. Our result shows that, using hot-press technique, which is generally less time consuming and very effective for making homogeneous sample, a large *ZT* value can be achieved with high mechanical strength.

In addition to this, the most interesting result we achieved is a decrement in the operating temperature value, with high $ZT \geq 1$. The ZT reported by Yang et al.[22] have values greater than 1.0 in the 380-390 K temperature range only. Additionally, in the low temperature phase, Yang et al. results below 360 K show ZT less than 0.8, and decrease continuously with decrease in temperature. This limitation on the high ZT value in a narrow temperature range restricts this material to a narrow temperature region for its optimal performance. With sulfur substitution, the resulting modifications in electrical resistivity and thermal conductivity allowed the material to achieve ZT values close to 1.0 in a wide temperature range. With a sulfur-substituted sample $Ag_2S_{0.4}Se_{0.6}$, we were able to achieve ZT equal to 1.08 at $\sim$ 350 K. Obtaining ZT = 1.08 with temperatures 40 K lower than those reported earlier is a great improvement in the thermoelectric properties of Ag_2Se-based material to be used for low temperature thermoelectric applications.

In addition to high ZT greater than 1.0 at about 350 K, $Ag_2S_{0.4}Se_{0.6}$ materials also possessed $ZT > 0.8$ down to room temperature. This is also a very important feature from the thermoelectric application point of view, and we successfully obtained it for this particular composition. With a material for which ZT is equal to unity or greater in the temperature range of 350–400 K, a thermoelectric module can be made, for example, where in different portions of the device, legs with different compositions can be connected in parallel to give better performance in the 350–400 K temperature range. From the application point of view, these results are very useful, as one can harvest the waste heat energy into useful electrical energy in a wide temperature range by a simple method of sulfur substitution in an Ag_2Se system.

CONCLUSIONS

We successfully synthesized a sulfur substituted Ag_2Se sample and investigated its thermoelectric properties in the 300–500 K temperature range. Using melt-cooling and hot press techniques, very good quality samples were synthesized. With sulfur substitution, a drop in phase transition temperature from 390 K (Ag_2Se) to 350 K for $Ag_2S_{0.4}Se_{0.6}$ was observed. All the samples showed n-type behavior. Electrical resistivity and magnitude of Seebeck coefficients decreased with temperature, and combined gave a large power factor with a maximum value of 5000 μW m^{-1} K^{-2} at 360 K for $Ag_2S_{0.2}Se_{0.8}$. With low magnitude of thermal conductivity ($\sim$ 0.6 W m^{-1} K^{-1}), low resistivity $\sim$ 1.8 mΩ cm, and large Seebeck coefficient ($\sim$ 184 μV/K), a value of ZT equal to 1.08 was obtained for an $Ag_2S_{0.4}Se_{0.6}$ sample at 350 K. The observed value of ZT for the same composition was greater than 0.8 in 300–350 K. Such high ZT

values at lower operating temperatures are very promising indicators for utilizing these materials for thermoelectric applications in regions of wide temperature variation.

CONFLICT OF INTERESTS

There is no conflict of interests.

ELECTRONIC SUPPLEMENTARY MATERIAL

The online version of this article (https://doi.org/10.1007/s11664-019-07879-z) contains supplementary material, which is available to authorized users.

REFERENCES

1. L.E. Bell, *Science* 321, 1457 (2008).
2. G.J. Snyder and E.S. Toberer, *Nat. Mater.* 7, 105 (2008).
3. P. Gorai, V. Stevanovic, and E.S. Toberer, *Nat. Rev. Mater.* 2, 17053 (2017).
4. L.L. Baranowski, G.J. Snyder, and E.S. Toberer, *Energy Environ. Sci.* 5, 9055 (2012).
5. G.J. Snyder, E.S. Toberer, R. Khanna, and W. Seifert, *Phys. Rev. B* 86, 045202 (2012).
6. Y. Pei, X. Shi, A. LaLonde, H. Wang, L. Chen, and G.J. Snyder, *Nature* 473, 66 (2011).
7. A.D. LaLonde, Y. Pei, H. Wang, and G.J. Snyder, *Mater. Today* 14, 526 (2011).
8. G.S. Nolas, J. Sharp, and H.J. Goldsmid, *Thermoelectrics, Basic Principles and New Materials Developments* (Berlin: Springer, 2001).
9. Y. Zhou and L.-D. Zhao, *Adv. Mater.* 29, 1702676 (2017).
10. R. Simon, R.C. Bourke, and E.H. Lougher, *Adv. Energy Convers* 3, 481 (1963).
11. M. Ferhat and J. Nagao, *J. Appl. Phys.* 88, 813 (2000).
12. C.H. Lee, Y.H. Park, and H. Hashimoto, *J. Appl. Phys.* 101, 024920 (2007).
13. Y.Z. Pei, N.A. Heinz, and G.J. Snyder, *J. Mater. Chem.* 21, 18256 (2011).
14. T. Day, F. Drymiotis, T.S. Zhang, D. Rhodes, X. Shi, L.D. Chen, and G.J. Snyder, *J. Mater. Chem. C* 1, 7568 (2013).
15. W.L. Mi, P.F. Qiu, T.S. Zhang, Y.H. Lv, X. Shi, and L.D. Chen, *Appl. Phys. Lett.* 104, 133903 (2014).
16. S. Kashida, N. Watanabe, T. Hasegawa, H. Iida, M. Mori, and S. Savrasov, *Solid State Ion.* 158, 167 (2003).
17. D. Byeon, R. Sobota, K.D. Codrin, S. Choi, K. Hirata, M. Adachi, M. Kiyama, T. Matsuura, Y. Yamamoto, M. Matsunami, and T. Takeuchi, *Nature Commun.* 10, 72 (2019).
18. H.Y. Yang, Y.W. Zhao, Z.Y. Zhang, H.M. Xiong, and S.N. Yu, *Nanotechnology* 24, 055706 (2013).
19. X. Shi, H. Chen, F. Hao, R. Liu, T. Wang, P. Qiu, U. Burkhardt, Y. Grin, and L. Chen, *Nat. Mater.* 17, 421 (2018).
20. F.D. Duman, I. Hocaoglu, D.G. Ozturk, D. Gozuacik, A. Kiraz, and H.Y. Acar, *Nanoscale* 7, 11352 (2015).
21. J. Pei, G. Chen, D. Jia, R. Jin, H. Xua, and D. Chena, *New J. Chem.* 37, 323 (2013).
22. D. Yang, X. Su, F. Meng, S. Wang, Y. Yan, J. Yang, J. He, Q. Zhang, C. Uher, M.G. Kanatzidis, and X. Tang, *J. Mater. Chem. A* 5, 23243 (2017).

23. J.A. Perez-Taborda, O. Caballero-Calero, L. Vera-Londono, F. Briones, and M. Martin-Gonzalez, *Adv. Energy Mater.* 8, 1702024 (2018).
24. Y. Ding, Y. Qiu, K. Cai, Q. Yao, S. Chen, L. Chen, and J. He, *Nat. Commun.* 10, 841 (2019).
25. G.A. Palyanova, R.G. Kravtsova, and T.V. Zhuravkova, *Russ. Geol. Geophys.* 56, 1738 (2015).
26. J.R. Carvajal, *Phys. B* 55, 192 (1993).
27. J.R. Carvajal, *Newsletter* 26, 12 (2001).
28. J. Hu, B. Deng, Q. Lu, K. Tang, R. Jiang, Y. Qian, G. Zhoua, and H. Chenga, *Chem. Commun.* 8, 715 (2000).
29. H. Billetter and U. Ruschewitz, *Z. Anorg. Chem.* 634, 241 (2008).
30. S.I. Sadovnikov and E. Yu, *Gerasimov Nanoscale Adv.* 1, 1581 (2019).
31. J. Liang, T. Wang, P. Qiu, S. Yang, C. Ming, H. Chen, Q. Song, K. Zhao, T. Wei, D. Ren, Y. Sun, X. Shi, J. He, and L. Chen, *Energy Environ. Sci.* 12, 2983 (2019).
32. G.A. Wiegers, *Am. Mineral.* 56, 1882 (1971).
33. R. Sadanaga and S. Sueno, *Muneralogical J.* 5, 124 (1967).
34. G.A. Palyanova, K.V. Chudnenko, and T.V. Zhuravkova, *Thermochim. Acta* 575, 90 (2014).